Bulletin of the Seismological Society of America, Vol. 96, No. 1, pp. 355–363, February 2006, doi: 10.1785/0120050019

Liquefaction Limit during Earthquakes and Underground Explosions: Implications on Ground-Motion Attenuation

by Chi-Yuen Wang, Alex Wong, Douglas S. Dreger, and Michael Manga

Abstract Liquefaction of saturated soils and sediments documented during earthquakes shows an empirical relation $\log R_{max} = 2.05\ (\pm 0.10) + 0.45\ M$, where R_{max} is the liquefaction limit in meters (i.e., the maximum distance from liquefaction site to the hypocenter) and M is the earthquake magnitude. Combining this with an empirical relation between M and the seismic energy of an earthquake, we obtain a relation between the liquefaction limit and the seismic energy: $E = A\ R_{max}^{\beta}$. The prefactor corresponds to a threshold energy for liquefaction ranging from 0.004 to 0.1 J/m^3; the exponent, ranging from 3.2 to 3.3, implies that the energy density of ground motion attenuates with distance according to $1/r^{3.2–3.3}$, where r is the distance from the hypocenter. The value of the threshold energy suggests a preliquefaction degradation of the shear modulus of soils by more than 3 orders of magnitude. Liquefaction documented during underground explosions is characterized by a threshold energy several orders of magnitude greater than that for liquefaction during earthquakes but shows a similar functional relation between E and R_{max} as that for liquefaction during earthquakes and implies a similar attenuation relation between ground-motion energy density and distance.

Introduction

Large earthquakes often cause saturated soils to lose their rigidity and become fluidlike—a phenomenon widely known as liquefaction and a major source of seismic hazard (Seed and Lee, 1966; Terzaghi *et al.*, 1996). Field and laboratory studies show that the occurrence of liquefaction depends on many factors, such as earthquake magnitude, shaking duration, peak ground motion (acceleration/velocity), depth to the groundwater table, basin structures, site effects and liquefaction susceptibility of sediments (e.g., Youd, 2003). Thus, the occurrence of liquefaction is difficult to predict on a theoretical basis; empirical approaches are adopted as a rule in assessing the liquefaction potential of an area. In engineering practices, the assessment method used most often is the ground-penetration test (e.g., Bardet, 2003). Such tests are usually applied at specific sites of engineering importance, even though in some metropolitan areas (e.g., Los Angeles and Memphis) penetration tests are widely applied to assess the liquefaction potential. On a broader scale, empirical relations between the magnitude of ground shaking and liquefaction (e.g., Wang *et al.*, 2003) may be combined with numerical simulations of ground shaking during an earthquake (e.g., Stidham *et al.*, 1999) to evaluate the liquefaction potential of a large area. Such application, however, requires extensive information about sediment properties and subsurface structures of the area of interest, and both are often unavailable.

In areas where such data are not available, a simpler approach may be applied to set some limits to the expected extent of liquefaction during potential earthquakes. Field observations show that, for earthquakes of a given magnitude M, the occurrence of liquefaction is confined within a particular distance from the earthquake focus, that is, the liquefaction limit, R_{max}, beyond which liquefaction may not be expected (e.g., Kuribayashi and Tatsuoka, 1975; Ambraseys, 1988; Papadopoulos and Lefkopulos, 1993; Galli, 2000). The liquefied sites at the liquefaction limit are likely to be those with the optimal conditions for liquefaction, that is, saturated soils with high liquefaction susceptibility. Thus the application of the liquefaction limit to an area without prior information on its liquefaction susceptibility may only be taken as an estimate of the maximum likelihood of liquefaction occurrence during a potential earthquake. Sites at closer distances may include less optimal conditions but are exposed to greater seismic input.

In this study we show, based on updated compilation of worldwide data, a new relation between the liquefaction limit and earthquake magnitude. This relation allows us to derive, for the first time, a relation between the liquefaction limit and the seismic energy, which in turn allows us to formulate an attenuation relation of seismic energy density with distance and to estimate the threshold seismic energy density required for soil liquefaction. By comparing these results with similar results for liquefaction during underground explosions, we attempt to decipher the differences and similarities between earthquake and underground explosion in their effects on soil liquefaction.

Liquefaction Limits

Kuribayashi and Tatsuoka (1975) compiled liquefaction data for Japan and showed that, for earthquakes of magnitude *M*, there was a limiting distance to the earthquake, that is, the liquefaction limit R_{max}, within which liquefaction may occur; they further showed that a linear relation may exist between *M* and log R_{max}. Ambraseys (1988) summarized worldwide liquefaction data from 1848 to 1980 and proposed a relationship among *M*, log R_{max}, and R_{max}; the inclusion of the last term resulted in a second-order correction to the linear relationship between *M* and log R_{max}. Papadopoulos and Lefkopulos (1993) found that a linear relation between *M* and log R_{max} provides a better fit to data for liquefaction in Greece. Galli (2000) also reported a linear relation between *M* and log R_{max} for liquefaction in Italy from both historical and instrumental records. These results are generally consistent with the understanding that the intensity of ground motion increases with earthquake magnitude and attenuates with epicentral distance. Although the attenuation of seismic energy is also known to be a function of the style of faulting (Boore *et al.*, 1997), the directivity of fault rupture (Sommerville *et al.*, 1997), and distance to the ruptured fault, the majority of reports on liquefaction did not document the directivity of the earthquake, the style of faulting, or the closest distance to the ruptured fault. We are therefore forced to use earthquake magnitude and hypocenter distance as the only two parameters to quantify the liquefaction limit. In a later section, however, we will argue that these two parameters may indeed be the most important in affecting liquefaction occurrence and may have embedded within themselves some other parameters as mentioned previously. Because a large amount of historical data is included in the present analysis, which did not make a distinction among different magnitude scales, we are forced to neglect the distinction among different magnitude scales. Estimate of the relationship between earthquake magnitude and liquefaction limit could also be made for prehistorical earthquakes (e.g., Obermeier, 1999), but the present analysis will be limited to historical and instrumental data.

By combining the aforementioned datasets and adding some recent liquefaction data (Table 1) we obtain a substantially larger dataset than any of the previous studies. Figure 1 shows the hypocentral distance of liquefaction against the earthquake magnitude *M*. For earthquakes of a given magnitude *M*, liquefaction generally occurs within a range of hypocentral distances. The maximum of this range is defined as the liquefaction limit R_{max}. A least-square fit of data for R_{max} versus *M* yields the following relation:

$$\log R_{max} = 2.05\ (\pm 0.10) + 0.45\ M, \tag{1}$$

where R_{max} is in meters and the standard error in determining R_{max} for a given earthquake magnitude is shown in the parentheses.

To relate R_{max} to the seismic-wave energy of an earthquake E_{eq}, we use the classical Gutenberg-Richter relation between E_{eq} and *M* (Gutenberg and Richter, 1956):

$$\log E_{eq} = 4.8 + 1.5\ M, \tag{2}$$

where E_{eq} is in joules. Another widely known relation between E_{eq} and *M* is by Bath (1966):

$$\log E_{eq} = 5.24 + 1.44\ M. \tag{3}$$

We use both (2) and (3) in the following analysis to provide an estimate of the uncertainty due to the uncertainty in the $M \sim E_{eq}$ relations. Combining (1) and (2) we obtain:

$$E_{eq} = A'\ R_{max}^{3.3}, \tag{4}$$

where $A' = 0.004–0.02\ J/m^3$. Combining (1) and (3) we obtain

$$E_{eq} = A''\ R_{max}^{3.2}, \tag{5}$$

where $A'' = 0.03–0.10\ J/m^3$. Thus the exponent in the E_{eq} versus R_{max} relation appears to be insensitive to the uncertainty in the $M \sim E_{eq}$ relations.

Liquefaction has also been documented in many underground explosions, both chemical (e.g., Ivanov, 1967; Charlie, 1978) and nuclear (e.g., Banister *et al.*, 1976; Blouin, 1978). Explosive compaction is commonly used to densify cohesionless soils and is known to induce local liquefaction (e.g., Green and Mitchell, 2004). Charlie *et al.* (1996) summarized these observations and obtained the following empirical relation existing between the liquefaction limit and the explosive yield of the explosions *Y*:

$$R_{max} = 260\ Y^{1/3}, \tag{6}$$

where *Y* is the yield of underground explosion in kilotons of TNT (kt) and R_{max} in meters. Or, in units of joule (1 kt $= 4.186 \times 10^{12}$ J), we have

$$R_{max} = 0.016\ Y^{1/3}. \tag{6'}$$

Using an empirical relation between the yield of underground explosion and the equivalent seismic magnitude for alluvium (Bolt, 1976), we may convert (6) to a relation between R_{max} and the equivalent seismic magnitude for underground explosions:

$$\log R_{max} = 0.28 + 0.44\ M. \tag{7}$$

Note that the slope of this relation is nearly identical with that in equation (1), whereas the intercept terms in the

Table 1
Maximum Epicentral Distance from Documented Liquefaction Sites and Focal Depth for Some Large Earthquakes Since 1983

Earthquake	Magnitude	Epicentral Distance (km)	Focal Depth (km)	Source
1983 Nihonkai-Chubu, Japan	7.7	160	15	http://www.ce.berkeley.edu/~hausler/sites/NKC001.pdf
1988 Udaipu Gahri, India	6.6	100	10	http://asc-india.org/gq/udaipur.htm
1989 Loma Prieta, California	7.1	93	18	Bardet and Kapuskar (1993)
1994 Northridge, California	6.7	50	19	www.lafire.com/famous_fires/940117_NorthridgeEarthquake/quake/02_EQE_geology.htm
1995 Manzanillo, Mexixo	7.3	150	30	http://sun1.pue.upaep.mx/servs/carrs/GIIS/manzanillo.html
1995 Kobe, Japan	6.9	40	10	http://www.jrias.or.jp/public/Hanshin_Earthquake/q1-2e.html
1999 Izmit, Turkey	7.8	61	17	Rothaus *et al.* (2004)
1999 Duzce, Turkey	7.5	56	10	http://geoinfo.usc.edu/turkey/
1999 Chi-Chi, Taiwan	7.6	80	8	Yu *et al.* (2000)
2001 Gujarat, India	7.7	260	17	Rajendran *et al.* (2001)
2001 Nisqually, Washington	6.8	75	52	Pierepiekarz *et al.* (2001)
2002 Denali, Alaska	7.9	300	4.2	Kayen *et al.* (2002)
2003 Colima, Mexico	7.7	60	30	http://geoinfo.usc.edu/gees/

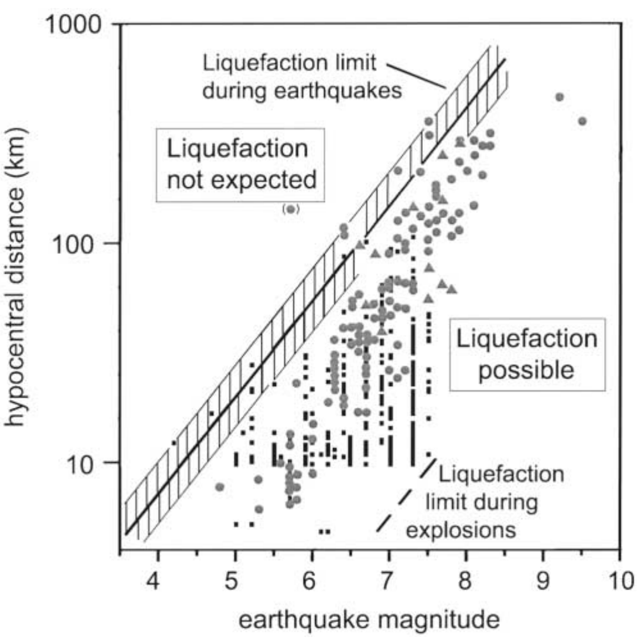

Figure 1. Diagram showing hypocentral distance of liquefaction documented during earthquakes versus earthquake magnitude. Different symbols show data from different sources: squares, Galli (2000); circles, Ambraseys (1988; including data in Kuribayashi and Tatsuoka [1975]); triangles, electronic supplement. Hypocentral distances are calculated from reported epicentral distance and focal depth; if focal depth is not reported, an average focal depth of 10 km is assumed. Solid line shows the liquefaction limit as a function of earthquake magnitude (equation 1); an outlier (in parentheses) has bare minimum information (Ambraseys, 1988) and is not included in the definition of the liquefaction limit. Dashed line shows the extrapolated relation between liquefaction limit and equivalent earthquake magnitude during underground explosions (equation 10).

two relations differ significantly (Fig. 1). This difference in intercept suggests that, at an equivalent M, the liquefaction limit for underground explosion is about two orders of magnitude smaller than that for earthquakes. This difference in the liquefaction limit is consistent with the general notion that shearing may be much more effective than compression in triggering liquefaction. Because most of the seismic energy generated by explosion occurs in compression, there is much less shear energy in explosions than in earthquakes of an equivalent magnitude. The difference in the liquefaction limit may also be due to a difference in the frequency content in ground motion between earthquake and explosion. Finally, the difference in the liquefaction limit between earthquake and underground explosion may be related to the difference in the duration of shaking which is known to affect the stress level for the occurrence of liquefaction (e.g., Seed and Lee, 1966); that is, the duration of ground shaking is much shorter during underground explosions than during earthquakes of an equivalent magnitude (e.g., Bolt, 1976). On the other hand, we caution that the liquefaction limits documented during explosions were all smaller than 1 km (i.e., the dash line in Fig. 1 is an extrapolation of the empirical relation from field data), whereas all the documented liquefaction limits during earthquakes were greater than 10 km (Fig. 1); hence, a strict comparison between (1) and (7) is necessarily fraught with uncertainty.

Most of the energy in underground explosions is spent in fracturing, heating, melting, and vaporizing the surrounding rocks (Bolt, 1976; Johnson and Sammis, 2001); only a very small fraction is converted to seismic energy. The fraction of the total energy that goes into seismic energy is a measure of the seismic efficiency of explosions, which ranges from 10^{-3} to 10^{-2} for sediments and solid rocks, respectively (Bolt, 1976). Assuming a seismic efficiency of 10^{-3} for sediments and soils we obtain from (6′) the seismic energy in underground explosions (E_{ex}),

$$E_{ex} \sim 240 \ R_{max}^3, \quad (8)$$

where E_{ex} is in joules.

Because equations (4), (5), and (8) all have the same functional form, we may summarize them into a single relation for the convenience of discussion:

$$E = A \ R_{max}^{\beta}, \quad (9)$$

where E is the seismic energy of the source and stands for either E_{eq} or E_{ex}, β ranges from 3 to 3.3, and A ranges from 0.004 to 0.1 J/m^3 for earthquakes and is ~240 J/m^3 for underground explosions.

Threshold Energy

We interpret R_{max} as the distance at which the seismic energy density $e(r)$, that is, the seismic energy in a unit volume, has decayed to a threshold energy density e_{th} (Fig. 2) required to trigger liquefaction of soils or sediments under the most favorable condition (i.e., saturated soils with high liquefaction susceptibility). What is this threshold energy density? In view of the functional form of (9), we assume the following functional form for the attenuation of ground-motion energy density with distance:

$$e(r) = \frac{E}{(r + 1)^{a}} \quad (10)$$

where r is the distance from the earthquake source in meters, E stands for either E_{eq} or E_{ex}, and α is an empirical constant to be determined; the term "+1" is included so that the seismic energy in a unit volume at $r = 0$, that is, $e(r = 0)$, is equal to the total seismic energy of the earthquake or underground explosion, that is, E. Replacing E in the preceding expression by the expression in (9) and r by R_{max}, we obtain the seismic-energy density at the liquefaction limit, that is, the threshold energy:

$$e_{th} \equiv e(R_{max}) = (A R_{max}^{\beta}) \ (R_{max} + 1)^{-\alpha} \sim (A R_{max}^{\beta}) \ R_{max}^{-\alpha}. \quad (11)$$

Because the threshold energy e_{th} is a soil property and should be independent of R_{max}, $\alpha = \beta$, which ranges from 3 to 3.3, and $e_{th} = A$, which ranges from 0.004 to 0.1 J/m^3 for liquefaction during earthquakes and is ~240 J/m^3 for liquefaction during underground explosions. The several orders of magnitude difference in the threshold energy between earthquakes and underground explosions is consistent with our earlier suggestion that the triggering of liquefaction during earthquakes and underground explosions is sensitive to the relative duration of ground shaking, the frequency content in ground motion, and the relative amount of shear energy in the induced ground motion.

Ground-Motion Attenuation

The previous analysis of liquefaction limit has led to the inference that the overall attenuation of the ground-motion energy density during earthquakes and underground explosions may follow the functional form

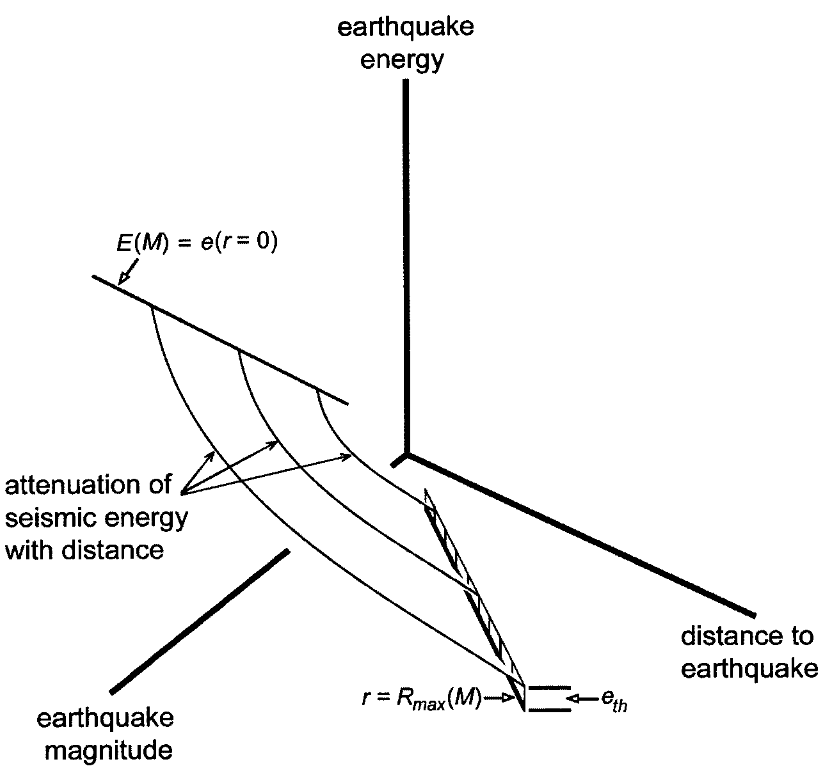

Figure 2. Schematic drawing illustrating the conceptual model of attenuation of the seismic energy with distance. $e(r)$ is the strong-motion energy in a unit volume at hypocentral distance r. At the earthquake source $e(r = 0) = E(M)$, which lies in the plane defined by the axes of earthquake energy E and earthquake magnitude M, and e_{th} is the threshold energy for liquefaction at $r = R_{max}$.

$$e(r) = \frac{E}{r^3} \sim \frac{E}{r^{3.3}}, \qquad (12)$$

where E is the total seismic energy in an earthquake or an underground explosion and r is the distance from the source.

Because ground-motion attenuation relationships have long been developed on seismological basis and widely used in seismic-hazard analysis, it would be interesting to compare the preceding relation based on liquefaction limit with the seismological relations. Most seismological attenuation relations describe the expected peak ground motions as a function of earthquake magnitude, distance to the source region, and local site characterization (Boore *et al.*, 1993, 1994; Abrahamson and Silva, 1997; Campbell, 1997). Some relations also include the style of faulting (Boore *et al.*, 1997) and directivity effects (Somerville *et al.*, 1997). A useful review is given by Campbell (2003). Numerous variables, such as basin effects (e.g., Graves *et al.*, 1998; Kawase, 1996), site effects (Campbell, 2003), and seismic waves, critically reflected off the Moho and other crustal layers (Somerville and Yoshimura, 1990; Catchings and Kohler, 1996), may cause significant changes in the ground-shaking intensity during any earthquake. Thus, it is difficult to determine how ground motion may attenuate with distance, and a wide variety of relations has been proposed. Boatwright *et al.* (2003) suggested that the peak ground acceleration (PGA) and the peak ground velocity (PGV) for nine large earthquakes and 95 moderate earthquakes in northern California may attenuate with distance more rapidly than a simple power law would predict, whereas Catchings and Kohler (1996) showed that the overall profile of the PGV along the San Francisco Peninsula during the 1989 Loma Prieta earthquake decreases according to $1/r^2$ for direct arrivals and $1/r$ for reflected arrivals. Applying an inversion scheme, Cua (2004) decomposed and parameterized the ground-motion envelopes of about 30,000 strong-motion records of Southern California earthquakes and developed the corresponding strong-motion attenuation relationships. The results show that, at soil sites, the amplitude of the horizontal S-wave velocity envelope declines with distance according to $\sim 1/r^{1.59}$. Because the amplitude of the horizontal S-wave velocity envelope usually corresponds to the horizontal PGV of the record, this result implies

$$\mathrm{PGV} \sim 1/r^{1.59}. \qquad (13)$$

Because of the large numbers of earthquakes used in Cua's (2004) study, we will compare the liquefaction-based attenuation relation against her result.

Although seismologists characterize the attenuation relationship by the decline of the PGA or PGV with distance, liquefaction of soils is caused by the cumulative deformation of saturated soils and sediments during ground shaking. Thus the attenuation relation (12) inferred from liquefaction limit represents the attenuation of the time-cumulative energy in the ground motion. To evaluate the cumulative ground-motion energy from the strong-motion records, we adopt the Arias intensity (Arias, 1970; Jennings, 2003) from earthquake engineering, which is a measure of the total amount of energy imparted to a spectrum of single-degree simple harmonic oscillators, that is,

$$e_{\mathrm{Ar}} = \int_0^\infty \int_0^\infty \ddot{u}(t)\ \dot{x}(\omega, t)\ dt\ d\omega \qquad (14)$$

where $x(\omega, t)$ is the displacement of a single-degree simple harmonic oscillator, of natural frequency ω, responding to (or driven by) ground acceleration $\ddot{u}(t)$ during an earthquake. In computing the response of the simple harmonic oscillators we assumed a 5% damping, following the usual practice in earthquake engineering. Plotting e_{Ar} against PGV for the 2004 M_w 6.0 Parkfield and the 2003 M_w 6.5 San Simeon, California, earthquakes (Fig. 3a, b) we obtain, respectively, the following linear relationships between log (e_{Ar}) and log (PGV),

$$\log e_{\mathrm{Ar}} = -1.24 + 1.82 \log \mathrm{PGV}, \qquad (15)$$

at $r^2 = 0.95$, and

$$\log e_{\mathrm{Ar}} = -1.66 + 2.04 \log \mathrm{PGV}, \qquad (16)$$

at $r^2 = 0.76$. These results demonstrate that e_{Ar} for horizontal S waves is closely proportional to the square of PGV. Thus the relationship $PGV \sim 1/r^{1.59}$ for horizontal S waves in Southern California (Cua, 2004) implies that the cumulative ground-motion energy density attenuates with distance according to $e \sim 1/r^3$ at soil sites. Thus the attenuation relationship from the present liquefaction limit study, (12), is consistent with the strong-motion records.

Ground motion during underground explosions has been documented both in the United States and in the then Soviet Union. Olsen and Peratt (1994) and Smith (1994) reported the ground motion during a 1-kt underground chemical explosion in the Nevada Test Site at distances up to 1 km, which may be characterized by a decline of PGV with distance according to $\sim 1/r^{1.6}$, and Kostyuchenko *et al.* (1974) reported the ground motion during nuclear explosions in central Asia at distances up to 100 km, which may be characterized by a decline of the PGV with distance according to $1/r^{1.75}$. The difference between these results may either reflect a real difference in the attenuation relations between the different tectonic regions, or it may simply reflect the uncertainty in the empirical relations. Assuming the same relation between PGV and the cumulative energy for ground motion during underground explosions, we may infer that the ground-motion energy density attenuates with distance according to $1/r^{3.2}$ for underground explosions in the Nevada Test Site, which is consistent with the attenuation relation (12) obtained on the ground of the liquefaction limit and according to $1/r^{3.5}$ for underground explosions in central Asia.

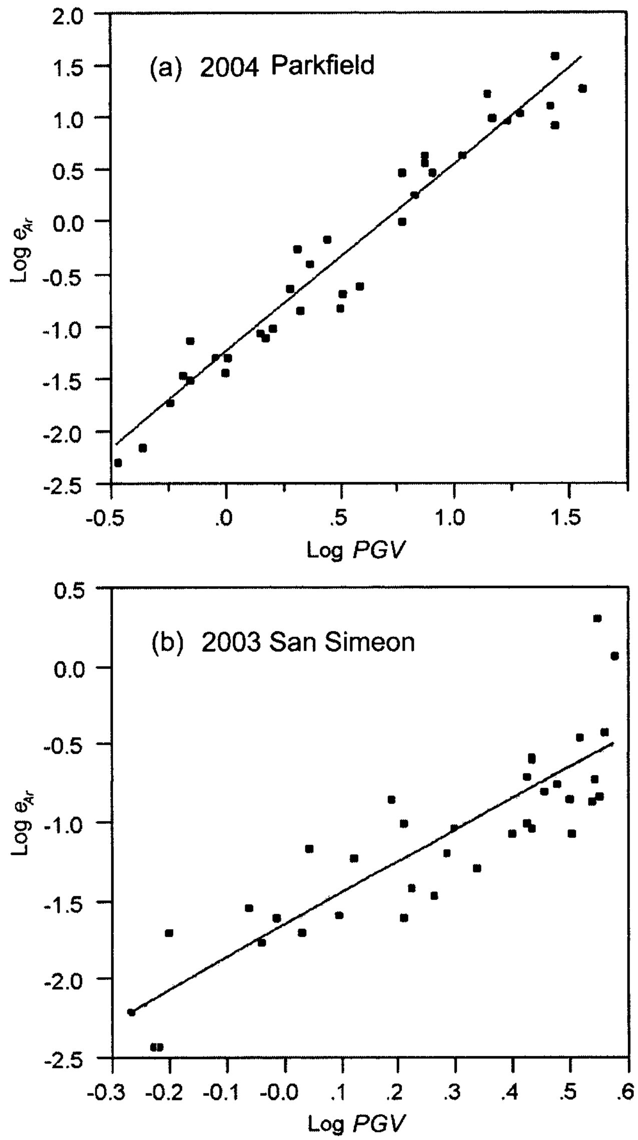

Figure 3. (a) Plot of logarithm of Arias intensity against logarithm of PGV of horizontal *S* waves for the 2004 Parkfield, California, earthquake. Straight line shows the best fit to data (see text). (b) Plot of logarithm of Arias intensity against logarithm of PGV of horizontal *S* waves for the 2003 San Simeon, California, earthquake. Straight line shows the best fit to data (see text).

Discussion

Because of the importance of liquefaction as a seismic hazard, a great deal of work has been done in earthquake engineering toward studying the liquefaction susceptibility of soils and sediments, and a large body of literature has been accumulated (e.g., National Research Council, 1985). In the field, numerous ground-penetration tests have been carried out in areas of engineering importance to assess the local liquefaction susceptibility (e.g., Bardet, 2003; Youd, 2003). In laboratories, numerous experiments with cyclic stresses were carried out to determine how various environmental factors may affect the occurrence of liquefaction in soils and sediments during earthquakes (e.g., Terzaghi *et al.*, 1996). These studies have resulted in a plethora of empirical liquefaction models (e.g., Martin *et al.*, 1975; Booker *et al.*, 1976; Finn, 1988; Byrne, 1991; Green, 2001). A review of these works would be beyond the scope of the present article. Thus, we shall only discuss a particular work which bears on the result of the present study. Green and Mitchell (2004) integrated experimental stress-strain hysteresis loops up to initial liquefaction and estimated an energy density of 0.03–0.19 kJ/m^3 required to induce liquefaction, which is 3 to 4 orders of magnitude greater than the threshold energy density estimated on the basis of the liquefaction limit. We interpret this difference because the liquefaction limits in Figure 1 and equation (1) are based on worldwide data and thus represent soil conditions with the optimal liquefaction susceptibility, whereas Green and Mitchell's result was for particular soils. Thus, for particular soils that may or may not have the optimal liquefaction susceptibility, the liquefaction limit (and the required energy density for liquefaction initiation) presented in this study may only be used to provide an estimate of the maximum likelihood of liquefaction occurrence during a potential earthquake.

A large amount of laboratory measurements for a variety of saturated soils under cyclic shearing, as summarized in Dobry *et al.* (1982) and Vucetic (1994), has shown that, pore pressure begins to increase at a shear-strain threshold of 10^{-4}. The shear-strain required for liquefaction appears to depend on soil density, effective stress, the number of stress cycles, and the duration of ground shaking (National Research Council, 1985), but, according to data compiled by Vucetic (1994), should be greater than 10^{-3}. Here we take 10^{-3} as the lower bound of the shear strain required for liquefaction to get a limiting estimate on the shear modulus of soils and sediments prior to liquefaction. We assume a simplified relation between the threshold energy for liquefaction and the threshold strain amplitude γ_{th}

$$e_{th} = \frac{1}{2} \mu_{eff} \gamma_{th}^2, \tag{17}$$

where μ_{eff} is an effective shear modulus at the threshold strain. Replacing e_{th} by its upper bound, that is, 0.1 J/m^3, and γ_{th} by its lower bound, that is, 10^{-3}, we obtain an upper-bound estimate of μ_{eff} of ~0.2 MPa, which is still more than 3 orders of magnitude smaller than the elastic shear moduli of sandy soils determined from shear-wave velocity measurements (Ishihara, 1996). This result implies that the shear modulus of soils and sediments may have degraded by more than 3 orders of magnitude during the earthquakes prior to the onset of liquefaction. This inference is in qualitative agreement with laboratory and field measurements. Laboratory experiments on saturated soils under cyclic loading have shown that soils weaken significantly once the increasing pore pressure reaches 0.5 of the confining pressure (De

Alba *et al.*, 1975; Luong, 1980). The magnitude of this degradation, however, may vary according to soil porosity, grain size, depth of burial, and geological age (National Research Council, 1985). Significant degradation of the rigidity of saturated soils were documented in the field during the 1987 Superstition Hills, California, earthquake, the 1989 Loma Prieta, California, earthquake, and the 1995 Kobe, Japan, earthquake, among others, prior to the occurrence of liquefaction (Holzer *et al.*, 1989; Pavlenko and Irikura, 2002; Ching and Glaser, 2003). Thus the small magnitude of the preliquefaction shear modulus, $\mu_{\rm eff}$, inferred from the threshold energy for liquefaction, is qualitatively consistent with the available field and laboratory measurements of soils and sediments under seismic and cyclic loading.

The small distance between the explosion-induced liquefaction and the explosion sources ($<$ 1 km; Charlie *et al.*, 1996) and the shallow depth of burial imply that the direct paths of the explosion-generated seismic waves must be shallow (e.g., Lay and Wallace, 1995). In view that the attenuation of earthquake-induced ground motion has the same functional form as that for explosion-induced ground motion we infer that the paths of the earthquake-induced seismic energy might also be shallow. This last inference appears to be consistent with the documented liquefaction during the 1987 Superstition Hills earthquake in Southern California, where the onset of pore-pressure buildup occurred with the arrival of amplified near-surface, near-station scattered waves (Holzer *et al.*, 1989).

Relation (1) implies that liquefaction would occur during earthquakes of any magnitude. However, no liquefaction has so far been documented for earthquakes with magnitudes smaller than 4 (see Fig. 1). This apparent paradox may have a simple explanation. Because most earthquakes occur at depths $\sim$10 km, $R_{\rm max}$ for earthquakes with magnitude smaller than 4 would be less than 10 km according to equation (1) and would thus be smaller than their focal depth. Consequently, no liquefaction might be expected at the surface for earthquakes with magnitude smaller than 4. In comparison, underground explosions are mostly conducted at shallow depths; liquefaction has been documented for explosions as small as 0.005 kt (Ivanov, 1967), with an equivalent magnitude of $\sim$2.

We stress that the liquefaction limit relation, that is, equation (1), includes only earthquake magnitude and distance to hypocenter as the parameters that influence liquefaction. Properties of the earthquake source (rupture directivity), properties of the seismic waves (frequency content), duration of ground shaking, properties of the region through which the waves travel (basin effect), and soil properties (liquefaction susceptibility) may all influence the occurrence of liquefaction. Although more work is needed to decipher the significance of each of these factors on the occurrence of liquefaction, we offer the following explanations of why some of these factors may not be required in defining the liquefaction limit in equation (1): (1) The liquefaction limit for a given earthquake magnitude (Fig. 1) is about an order of magnitude greater than the corresponding fault length, as estimated from empirical relations between fault length and magnitude (e.g., Kanamori and Anderson, 1975). Thus at the distances of the liquefaction limit, the rupture directivity on a fault may be a secondary factor, relative to earthquake magnitude and hypocentral distance, in affecting the occurrence of liquefaction. (2) For earthquakes of the same magnitude, the variations in some factors, such as frequency content and the duration of ground shaking, may be small enough that their effect on the occurrence of liquefaction is "hidden" in the magnitude parameter. (3) The soil condition at the liquefaction limit may represent an optimal liquefaction susceptibility, as noted earlier.

In conclusion, we showed, based on updated compilation of global data, an empirical relation between the liquefaction limit $R_{\rm max}$ of saturated soils and earthquake magnitude M. Combining this relation with a relation between M and the seismic energy of an earthquake, we derived a relation between $R_{\rm max}$ and the seismic energy: $E = AR^{\beta}_{\rm max}$. The exponent of this relation implies that the cumulative ground-motion energy density attenuates with distance according to $\sim 1/r^3$. The value of the prefactor corresponds to a threshold energy for liquefaction and implies a preliquefaction degradation of the shear modulus of soils by 3 to 4 orders of magnitude. By utilizing Cua's (2004) attenuation relationship derived from $\sim$30,000 strong-motion records for Southern Californian earthquakes, together with the records for the 2004 Parkfield earthquake and the 2003 San Simeon earthquake, we demonstrate that the implication of the liquefaction limit relationship, that the cumulative ground-motion energy density attenuates with distance according to $\sim 1/r^3$, is consistent with strong-motion records. Liquefaction documented during underground explosions is characterized by a threshold energy several orders of magnitude greater than that for liquefaction during earthquakes, but it shows a functional relation between E and $R_{\rm max}$ similar to that for liquefaction during earthquakes and implies a similar attenuation relation between ground-motion energy density and distance.

Acknowledgments

We thank Bruce Bolt for suggesting the durations of ground shaking may be a significant factor in affecting the difference in liquefaction during earthquakes and underground explosions, Lane Johnson for referring us to works on seismic wave attenuation in explosions, Wayne Charlie for referring us to works on explosion-induced liquefaction, Georgia Cua for referring us to her Ph.D. thesis and related work, and an anonymous reviewer for useful comments. Research was supported by NSF Geosciences (EAR-0125548) and NASA Astrobiology Institute (NNA04CC02A).

References

Abrahamson, N. A., and W. J. Silva (1997). Empirical response spectral attenuation relationships for shallow crustal earthquakes, *Seism. Res. Lett.* **68,** 94–127.

Ambraseys, N. N. (1988). Engineering seismology, *Earthquake Eng. Struct. Dyn.* **17,** 1–105.

Arias, A. (1970). A measure of earthquake intensity, in *Seismic Design for Nuclear Power Plant*, R. J. Hansen (Editor), Massachusetts Institute of Technology, Cambridge, Massachusetts, 438–483.

Banister, J. R., R. Pyke, D. M. Ellett, and L. Winters (1976). In-situ pore pressure measurements at Rio Blanco, *J. Geotech. Eng. Div. (Am. Soc. Civ. Eng.)* **102,** 1073–1091.

Bardet, J. P. (2003). Advances in analysis of soil liquefaction during earthquakes, in *International Handbook of Earthquake and Engineering Seismology, Part B*, W. H. K. Lee, H. Kanamori, P. C. Jennings, and C. J. Kisslinger (Editors), Academic Press, Amsterdam, 1175–1201.

Bardet, J. P., and M. Kapuskar (1993). Liquefaction sand boil in San Francisco during 1989 Loma Prieta earthquake, *J. Geotech. Eng.* **119,** 543–562.

Bath, M. (1966). Earthquake energy and magnitude, *Phys. Chem. Earth* **7,** 115–165.

Blouin, S. (1978). Liquefaction evidence observed in various explosive events, Transcripts of International Workshop on Blast-induced Liquefaction, London and U.S. Air Force Office of Scientific Research, Maidenhead, United Kingdom, 95–110.

Boatwright, J., H. Bundock, J. Luetgert, L. Seekins, L. Gee, and P. Lombard (2003). The dependence of PGA and PGV on distance and magnitude inferred from northern California ShakeMap Data, *Bull. Seism. Soc. Am.* **93,** 2043–2055.

Bolt, B. A. (1976). *Nuclear Explosions and Earthquakes: The Parted Veil*, W. H. Freeman, San Francisco, 309 pp.

Booker, J. R., M. S. Rahman, and H. B. Seed (1976). *GADFLEA—A Computer Program for the Analysis of Pore Pressure Generation and Dissipation during Cyclic or Earthquake Loading, EERC 76-24*, University of California, Berkeley.

Boore, D. M., W. B. Joyner, and T. E. Fumal (1993). Estimation of response spectra and peak accelerations from western North American earthquakes: an interim report, *U.S. Geol. Surv. Open-File Rept. 93-509*, Menlo Park, California.

Boore, D. M., W. B. Joyner, and T. E. Fumal (1994). Estimation of response spectra and peak accelerations from western North American earthquakes: an interim report, Part 2, *U.S. Geol. Surv. Open-File Rept. 94-127*, Menlo Park, California.

Boore, D. M., W. B. Joyner, and T. E. Fumal (1997). Equations for estimating horizontal response spectra and peak acceleration from western North American earthquakes: a summary of recent work, *Seism. Res. Lett.* **68,** 128–153.

Byrne, P. M. (1991). A cyclic shear-volume coupling and pore pressure model for sand, in *Proceedings: Second International Conference on Recent Advances in Geotechnical Earthquake Engineering and Soil Dynamics*, St. Louis, Missouri, 11–15 March 1991, 47–55.

Campbell, K. W. (1997). Empirical near-source attenuation relationships for horizontal and vertical components of peak ground acceleration, peak ground velocity, and pseudo-absolute acceleration response spectra, *Seism. Res. Lett.* **68,** 154–179.

Campbell, K. W. (2003). Strong-motion attenuation relations, in *International Handbook of Earthquake and Engineering Seismology, Part B*, Academic Press, Amsterdam, 1003–1012.

Catchings, R. D., and W. M. Kohlers (1996). Reflected seismic waves and their effect on strong shaking during the 1989 Loma Prieta, California, earthquake, *Bull. Seism. Soc. Am.* **86,** 1401–1416.

Charlie, W. A. (1978). The Dial Pack Event, Transcripts of International Workshop on Blast-induced Liquefaction, London and U.S. Air Force Office of Scientific Research, Maidenhead, United Kingdom, 149–165.

Charlie, W. A., G. E. Veyera, D. S. Durnford, and D. O. Doehring, (1996). Porewater pressure increases in soil and rock from underground chemical and nuclear explosions, *Eng. Geol.* **43,** 225–236.

Ching, J., and S. D. Glaser (2003). Identification of soil degradation during earthquake excitations by Bayesian inference, *Earthquake Eng. Struct. Dyn.* **32,** 845–869.

Cua, G. B. (2004). Creating the virtual seismologist: developments in ground motion characterization and seismic early warning, *Ph.D. dissertation*, Caltech, 408 p.

De Alba, D. P., C. K. Chan, and H. B. Seed (1975). Determination of soil liquefaction characteristics by large-scale laboratory tests, EERC Rpt. 75-14, College of Engineering, University of California, Berkeley, 153 p.

Dobry, R., R. S. Ladd, F. Y. Yokel, R. M. Chung, and D. Powell (1982). Prediction of pore water pressure buildup and liquefaction of sands during earthquakes by the cyclic strain method, *NBS Building Sci. Ser. U.S.* **138**.

Finn, W. D. L (1988). Dynamic analysis in geotechnical engineering, in *Earthquake Engineering and Soil Dynamics II—Recent Advances in Ground-Motion Evaluation*, J. L. von Thun (Editor), *ASCE Geotechnical Special Publication 20*, 523–591.

Galli, P. (2000). New empirical relationships between magnitude and distance for liquefaction, *Tectonophysics* **324,** 169–187.

Graves, R. W., A. Pitarka, and P. G. Somerville (1998). Ground motion amplification in the Santa Monica area: effect of shallow basin edge structure, *Bull. Seism. Soc. Am.* **88,** 1224–1242.

Green, R. A. (2001). *Energy-based evaluation and remediation of liquefiable soils*, *Ph.D. dissertation*, Virginia Polytechnical Institute and State University, 397 pp.

Green, R. A., and J. K. Mitchell (2004). Energy-based evaluation and remediation of liquefiable soils, *Geotech. Eng. Transp. Proj.* **2,** 1961–1970.

Gutenberg, B., and C. F. Richter (1956). Earthquake magnitude, intensity energy and acceleration, *Bull. Seism. Soc. Am.* **46,** 105–145.

Holzer, T. L., J. C. Tinsley, and T. C. Hank (1989). Dynamics of liquefaction during the 1987 Superstition Hills, California, earthquake, *Science* **244,** 56–59.

Ishihara, K. (1996). *Soil Behaviour in Earthquake Geotechnics*, Oxford University Press, Oxford, 350 pp.

Ivanov, P. L. (1967). Comparison of noncohesive soils by explosions, Izdatel'sstvo Literatury Po Stroietl'stvu, Leningrad, U.S.S.R., translated by the Indian National Scientific Documentation Center, New Dehli, India, published for the U.S. Department of Interior, Bureau of Reclamation and National Science Foundation, Washington, D.C. 211 pp.

Jennings, P. C. (2003). An introduction to the earthquake response of structures, in *International Handbook of Earthquake and Engineering Seismology, Part B*, Academic Press, Amsterdam, 1097–1125.

Johnson, L. R., and C. G. Sammis (2001). Effects of rock damage on seismic waves generated by explosions, *Pure Appl. Geophys.* **158,** 1869–1908.

Kayen, R., E. Thompson, D. Minasiah, B. Collins, E. R. S. Moss, N. Sitar, and G. Carver (2002). Geotechnical reconnaissance of the November 3, 2002 M7.9 Denali fault earthquake, *Earthquake Spectra*, Special Issue on the M7.9 Denali Fault Earthquake of 3 November 2002, 1–27.

Kawase, H. (1996). The cause of damage belt in Kobe, the 'basin-edge effect,' constructive interference of the direct s-wave with the basin-induced diffracted/Rayleigh waves, *Seism. Res. Lett.* **67,** 25–34.

Kostyuchenko, V. N., V. Rodionov, and D. Sultanov (1974). Seismic waves of underground nuclear explosions, in *Peaceful Nuclear Explosions III*, International Atomic Energy Agency, Vienna, 447–461.

Kuribayashi, E., and F. Tatsuoka (1975). Brief review of liquefaction during earthquakes in Japan, *Soil Found.* **15,** 81–92.

Lay, T., and T. C. Wallace (1995). *Modern Global Seismology*, Academic Press, San Diego, 521 pp.

Luong, M. P. (1980). Stress-strain aspects of cohesionless soils under cyclic and transient loading, in G. N. Pande and O. C. Zienkiewicz (Editors), *Proc. Intern. Symp. Soils under Cyclic and Transient Loading*, A.A. Balkema, Rotterdam, Netherlands, 315–324.

Martin, G. R., W. D. L. Finn, and H. B. Seed (1975). Fundamentals of liquefaction under cyclic loading, *Geotech. Eng. Div.* (*Am. Soc. Civ. Eng.*) **101,** no. GT5, 423–438.

National Research Council (1985). *Liquefaction of Soils during Earthquakes*, National Academy Press, Washington, D.C., 240 pp.

Obermeier, S. F. (1999). Liquefaction evidence for strong earthquakes of Holocene and Latest Pleistocene ages in the states of Indiana and Illinois, USA, *Eng. Geol.* **50,** 227–254.

Olsen, K. H., and A. L. Peratt (1994). Free-field gound motion for the nonproliferation experiment: preliminary comparisons with nearby nuclear events, in *Proc. Symp. on the Non-Proliferation Experiments (NPE): Results and Implications for Test Ban Treaties*, M. D. Denny (Editor), CONF-9404100 Department of Energy, 283–297.

Papadopoulos, G. A., and G. Lefkopulos (1993). Magnitude-distance relations for liquefaction in soil from earthquakes, *Bull. Seism. Soc. Am.* **83,** 925–938.

Pavlenko, O., and K. Irikura (2002). Changes in shear moduli of liquefied and nonliquefied soils during the 1995 Kobe earthquake and its aftershocks at three vertical-array sites, *Bull. Seism. Soc. Am.* **92,** 1952–1969.

Pierepiekarz, M. R., D. B. Ballantyne, and R. O. Hamberger (2001). Damage report from Seattle, *Civ. Eng.* (*Am. Soc. Civ. Eng.*) **71,** 78–83.

Rajendran, K., C. P. Rajendran, M. Thakkar, and M. P. Tuttle (2001). The 2001 Kutch (Bhuj) earthquake: coseismic surface features and their significance, *Curr. Sci.* **80,** 1397–1405.

Rothaus, R. M., E. Reinhardt, and J. Noller (2004). Regional consideration of coastline change, tsunami damage and recovery along the southern coast of the Bay of Izmit, *Nat. Hazards* **31,** 233–252.

Seed, H. B., and K. L. Lee (1966). Liquefaction of saturated sands during cyclic loading, *J. Soil Mech. Found. Div.* **92,** 105–134.

Smith, C. W. (1994). NPE—close-in stress and motion measurements, in *Proc. Symp. on the Non-Proliferation Experiments* (*NPE*): *Results and Implications for Test Ban Treaties*, M. D. Denny (Editor), CONF-9404100 Department of Energy, 254–270.

Somerville, P. G., and J. Yoshimura (1990). The influence of critical Moho reflections on strong ground motion records in San Francisco and Oakland during the 1989 Loma Prieta earthquake, *Geophys. Res. Lett.* **17,** 1203–1206.

Somerville, P. G., N. F. Smith, R. W. Graves, and N. A. Abrahamson (1997). Modification of empirical strong ground motion attenuation relations to include the amplitude and duration effects of rupture directivity, *Seism. Res. Lett.* **68,** 199–222.

Stidham, C., M. Antolik, D. Dreger, S. Larsen, and B. Romanowicz (1999). Three-dimensional structure influences on the strong-motion wavefield of the 1989 Loma Prieta earthquake, *Bull. Seism. Soc. Am.* **89,** 1184–1202.

Terzaghi, K., R. B. Peck, and G. Mesri (1996). *Soil Mechanics in Engineering Practice*, Third Ed., John Wiley & Sons, New York, 549 pp.

Vucetic, M. (1994). Cyclic threshold shear strains in soils, *J. Geotech. Eng.* **120,** 2208–2228.

Yu, M.-S., B.-C. Shieh, and Y. T. Chung (2000). Liquefaction induced by Chi-Chi earthquake on reclaimed land in central Taiwan, *Sino-Geotech.* **77,** 39–50 (in Chinese).

Wang, C. Y., D. S. Dreger, C.-H. Wang, D. Mayeri, and J. G. Berryman (2003). Field relations among coseismic ground motion, water level change and liquefaction for the 1999 Chi-Chi ($M_w = 7.5$) earthquake, Taiwan, *Geophys. Res. Lett.* **30,** no. 17, 1890, doi 10.1029/2003 GL017601.

Youd, T. L. (2003). Liquefaction mechanisms and induced ground failure, in *International Handbook of Earthquake and Engineering Seismology, Part B*, W. H. K. Lee, H. Kanamori, P. C. Jennings, and C. J. Kisslinger (Editors), Academic Press, Amsterdam, 1159–1173.

Department of Earth and Planetary Science
University of California
Berkeley, California 94720

Manuscript received 28 January 2005.